

2D-1D Coupling in Cleaved Edge Overgrowth

R. de Picciotto,¹ H. L. Stormer,^{1,2} A. Yacoby,^{1,3} L. N. Pfeiffer,¹ K. W. Baldwin,¹ and K. W. West¹

¹*Bell-Labs, Lucent Technologies, Murray Hill, New Jersey 07974*

²*Department of Physics and Department of Applied Physics, Columbia University, New York, New York 10003*

³*Braun Center for Submicron Research, Department of Condensed Matter Physics, Weizmann Institute of Science, Rehovot 76100, Israel*

(Received 3 April 2000)

We study the scattering properties of an interface between a one-dimensional (1D) wire and a two-dimensional (2D) electron gas. Experiments were conducted in the highly controlled geometry provided by molecular beam epitaxy overgrowth onto the cleaved edge of a high quality GaAs/AlGaAs quantum well. Such structures allow for the creation of variable length 1D-2D coupling sections. We find ballistic 1D electron transport through these interaction regions with a mean free path as long as $6 \mu\text{m}$. Our results explain the origin of the puzzling nonuniversal conductance quantization observed previously in such 1D wires.

PACS numbers: 73.20.Dx, 73.23.Ad

A perfect one-dimensional (1D) wire with ideal contacts at both ends is expected to exhibit a quantized conductance in multiples of the universal value $g_0 = 2e^2/h$. As successive 1D electronic subbands are filled with electrons the conductance increases in a series of steps with plateau values equal to g_0 multiplied by the number of occupied wire modes. This behavior is unique to 1D and does not occur in higher dimensions [1–12].

Wires fabricated in the GaAs/AlGaAs material system via the cleaved edge overgrowth (CEO) technique [13–16] represent one of the most precise implementations of the 1D concept. Such structures are controlled to atomic precision, leading to very uniform electron confinement with subband spacings as large as 25 meV. In addition, the cleanliness of the molecular beam epitaxy (MBE) environment results in wires with a backscattering mean free path, l_B , as long as $20 \mu\text{m}$. Indeed such wires show well-quantized conductance plateaus. However, surprisingly, the values of the measured conductances fall short of the universal values by as much as 25%. This behavior is observed in wires much shorter than l_B [13,16], implying that 1D backscattering alone cannot account for this deficit. Instead, it has been suggested that the observed nonuniversality is associated either with electron scattering between the 1D wire and its 2D contacts [13,17] or with disorder combined with e - e interactions in the wire [13,16,18].

An ideal Ohmic contact to a conductor should fill all outgoing states up to an electrochemical potential μ and absorb all incoming particles [1]. In 1D such an ideal contact takes the form of an adiabatic funnel—slowly reducing the cross section of a two- or three-dimensional conductor until the 1D wire is formed at its end. The adiabaticity of the dimensional changeover avoids reflections at the entrance to the wire and thus ensures filling of all the outgoing states [6]. Nearly adiabatic funnels can be fabricated in semiconductor structures by using two lithographically defined gates to progressively narrow a two-dimensional electron gas (2DEG) in order to form a wire

[19]. When the distance between the funnels is shrunk to a point, as in quantum point contacts, essentially quantized conductance values can be observed [20,21]. However, 1D wires of a finite length that are fabricated by lithography suffer from small 1D subband energy separation leading to possible mode mixing. Moreover, random width fluctuations can create discrete quantum point contacts along the wire that may dominate the conductance.

In CEO the 1D wire is contacted via a 2DEG, as illustrated in Fig. 1. While this figure displays the more complex three terminal CEO device to be addressed later, it contains all the ingredients of a generic 2DEG contact to a

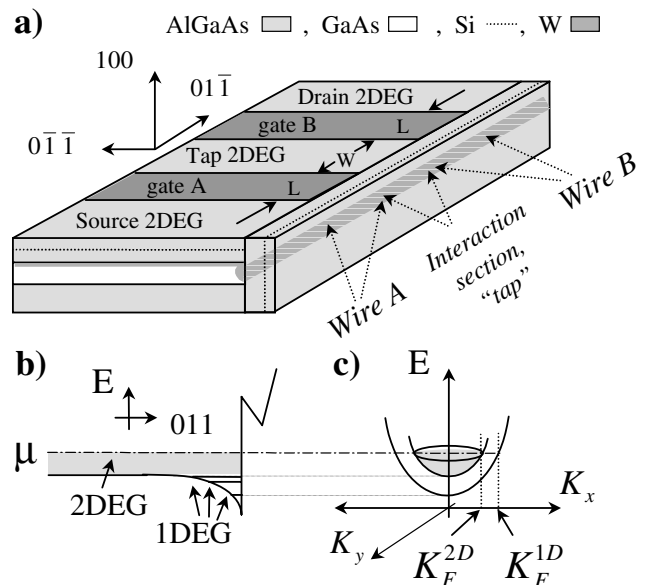


FIG. 1. (a) The geometry of the CEO device; see text. (b) Conduction band profile in the $[011]$ direction at the quantum well level away from gates A and B. The 2DEG and the 1DEG modes are illustrated. (c) Dispersion relation for electrons in the 2DEG and 1D wire. The Fermi wave vectors of the two systems are indicated.

CEO wire. Its fabrication starts with a high quality 2DEG created by MBE growth of a unilaterally doped GaAs quantum well (QW) onto a [001] GaAs substrate. The resultant 2DEG has a carrier density $n_s \approx 2.5 \times 10^{11} \text{ cm}^{-2}$, and mobility $\mu \approx 4 \times 10^6 \text{ cm}^2/\text{Vs}$. Subsequently, this wafer is cleaved inside the MBE chamber to expose a clean and atomically smooth [110] surface, which is immediately overgrown with a modulation-doped epitaxial layer sequence. The additional remote Si dopants that are introduced by this overgrowth step lead to a higher electron density near the cleaved edge of the QW. As in conventional modulation-doped samples, a strong built-in electric field binds this excess charge to the cleaved edge interface, creating 1D bound states all along the edge of the GaAs QW. This channel contains ~ 10 electronic modes and is referred to as the "1DEG." The 2DEG, residing in the QW plane, couples to the 1DEG from the side.

To separate the 2DEG from the 1DEG, a prefabricated tungsten gate electrode (e.g., gate A in Fig. 1) is used to deplete the 2DEG from underneath it, leaving only the 1D channel in this region along the edge. We refer to this isolated 1D channel in front of the gate as the "wire." The width of the tungsten gate defines the length L of the wire. The 2DEGs on both sides function as contacts. Increasing the gate voltage beyond depletion of the 2DEG provides a convenient tool to control the number of occupied 1D-wire modes. In this geometry, the 1DEG is coupled to the 2DEG on either side of the wire for practically an infinite length. Such extensive overlap seems to insure efficient electron transfer. However, an electron that is transferred from the 2DEG into the 1DEG far away from the entrance to the wire might backscatter within the 1DEG or scatter back into the 2DEG. Therefore, a combination of l_B and the 2D-1D scattering length, $l_{2D \rightarrow 1D}$, establishes an effective contact length which affects the efficiency with which the outgoing 1D states are filled by the 2DEG source. Such a reduced contact emissivity gives rise to a larger contact resistance which, in a two terminal (2T) measurement, subtracts from the ideal quantized conductance value. To elucidate whether such interplay between both scattering processes accounts for the conduction deficit observed in CEO wires requires a determination of these length scales, which is the focus of our investigation.

Study of the 2D-1D scattering length requires a well-defined, controllable geometry. This can be achieved by splitting the top tungsten gate in two [gates A and B in Fig. 1(a)], creating between the gates a section of controllable length, W , where a 2DEG strip interacts with the 1DEG. In such a geometry, electrons are injected from the 2DEG into the 1DEG in the source region and travel ballistically through the short wire in front of gate A. The electrons then proceed into the 1DEG in the central tap region, where they interact with a floating 2DEG for a length W before entering wire B and finally reaching the drain. Such a geometry allows one to determine the length scale

over which the 2DEG reservoir couples efficiently to the 1DEG and a good contact is formed [1,3].

Transport data for such a device at a temperature of $\theta \approx 300 \text{ mK}$ are shown in Fig. 2. The 2T conductance, g_1 , through a $\sim 2 \mu\text{m}$ long wire A is shown by the dashed line in this figure. Equivalent results are obtained for wire B (not shown). For these measurements a single gate (A or B) is activated. We observe clear conductance plateaus with a step height of $g_1 \approx 0.8g_0$, about 20% smaller than the expected value g_0 . With both gates activated, we measure the overall conductance, g_2 , of both wires plus the (floating) tap in series. Here, gate B is used to establish a single 1D mode in wire B while the voltage applied to gate A is scanned. The solid line in the inset of Fig. 2 shows the result for a $W \sim 10 \mu\text{m}$ long tap. When both wires support a single mode we find $g_2 \approx 0.4g_0 \approx \frac{1}{2}g_1$ (Fig. 2 inset, shaded area). This indicates complete 1D momentum randomization in the tap, leading to an Ohmic combination of the resistances of the two wires in series. The same measurement with a short tap, $W \sim 2 \mu\text{m}$, leaves the overall conductance nearly unaltered, $g_2 \approx 0.75g_0 \approx 0.94g_1$ (Fig. 2, shaded area). This clearly demonstrates ballistic 1D transport through the $2 \mu\text{m}$ long tap. For an intermediate tap length

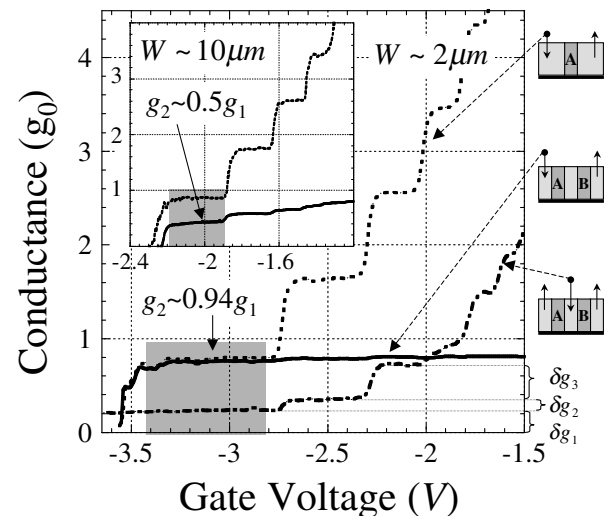


FIG. 2. Two terminal conductances of the junction. Dashed line: conductance, g_1 , of the $2 \mu\text{m}$ long wire A, plotted against the voltage applied to gate A. Solid line: conductance, g_2 , of two wires in series with a $2 \mu\text{m}$ long floating tap plotted versus the voltage applied to gate A, while wire B sustains only one mode. Dashed-dotted line: conductance, g_1 , from a $2 \mu\text{m}$ long tap into both sides of the junction plotted versus the voltage applied to gate A, while wire B sustains only one mode. The contributions of the first three modes, δg_i , are indicated. The experimental setups used for the various measurements are sketched. Arrows correspond to current flow direction, and points correspond to a voltage measurement port. The shaded regions correspond to a single mode in both wires A and B. A standard lock-in technique with an excitation current smaller than 1 nA at a temperature, $\theta \approx 300 \text{ mK}$ was used. Inset: g_1 and g_2 (same as main figure) for a $10 \mu\text{m}$ long tap.

of $W \sim 6 \mu\text{m}$ we find $g_2 \approx 0.6g_0 \approx 0.75g_1$ (not shown). This value falls about halfway between the ‘‘Ohmic tap’’ result, $\frac{1}{2}g_1$, and the ‘‘no tap’’ value, g_1 .

The smaller value of g_2 as compared to g_1 is directly related to backscattering in the 1D that is induced by the tap. Seemingly, 1D backscattering might be modified by the mere presence of the tap even *without* 2D-1D charge transfer. However, e - e scattering that involves momentum exchange without charge transfer *cannot* occur since $k_F^{2D} < k_F^{1D}$ [see Figs. 1(b) and 1(c)]. Further, k_F^{2D} is too small for efficient screening of the disorder potential by the 2DEG at the wave vectors relevant for 1D backscattering. The backscattering length in a wire, l_B^{wire} , is therefore expected to be very similar to the backscattering length in the 1DEG, $l_B^{1\text{DEG}}$. Thus, the smaller value of g_2 is directly related to charge transmission across the 1D-2D interface, or to the *invasiveness* of the tap [3]. Since this 2DEG is floating, each electron that scatters from the 1DEG into the 2DEG at the tap is replaced by an electron that scatters in the reverse direction. This latter electron, however, has an equal probability to scatter into either direction; $+k_F^{1D}$ or $-k_F^{1D}$ and the momentum of the original electron are completely lost on average. Thus, the longer the tap is, the more invasive it is, and the more it induces 1D momentum loss, leading to a smaller value of g_2 . Our measurements thus determine a 2D-1D mean free path of $l_{2D \leftrightarrow 1D} \approx 6 \mu\text{m}$.

The 2D-1D scattering length establishes the quality of the contacts and hence determines the 2T conductance g_1 . A theoretical model [13] for a 1D wire placed between 2DEG contacts derives an expression for the 2T conductance $g_1 = g_1(1 + 2l_{2D \leftrightarrow 1D}/l_B^{1\text{DEG}})^{-1/2}$ in terms of the two length scales $l_B^{1\text{DEG}}$ and $l_{2D \leftrightarrow 1D}$. Our measurements determine directly $l_{2D \leftrightarrow 1D}$, which was not possible in any of the previous 2T measurements. Using $l_{2D \leftrightarrow 1D} \approx 6 \mu\text{m}$ and the 1D backscattering length $l_B^{1\text{DEG}} \approx l_B^{\text{wire}} \approx 20 \mu\text{m}$ in such wires [13] and placing it in the above expression yields $g_1 = (0.79 \pm 0.04)g_0$ for the 2T conductance [22]. The so-derived 2T conductance value is in excellent agreement with our *measured* 2T conductance of $g_1 \approx 0.8g_0$. Our result demonstrates that the origin of the nonuniversal conductance in CEO wires is 2D-1D scattering in the contact regions. This is the central finding of our measurements. Beyond CEO wires, such considerations are relevant for standard contact schemes, generally used for one-dimensional molecules [23–26], where electrons are envisioned to enter and leave the wire ‘‘all along the length’’ of some evaporated contacts.

Our device allows us to perform three terminal (3T) measurements on a wire by using the tap as a third terminal. Thus far, such measurements, with a weakly invasive third port, have not been possible in 1D systems. As an example, we show the result of a particular 3T configuration in Fig. 3. The current is driven from the center tap and sunk solely at the drain, while the source is

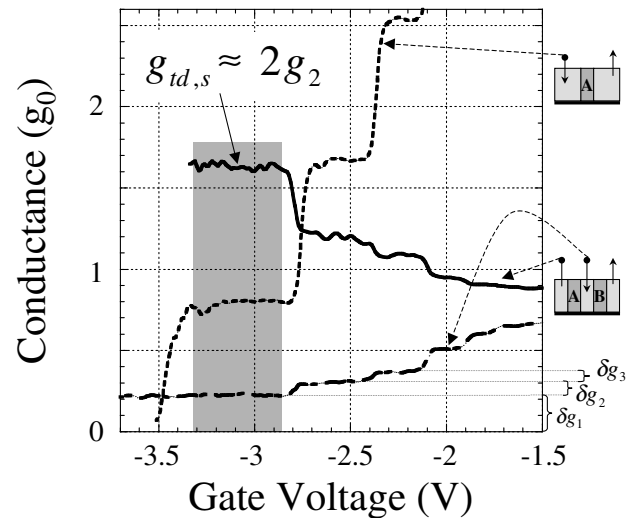


FIG. 3. A three terminal conductance measurement. A current, I_t , is driven from a $2 \mu\text{m}$ long tap to the drain while both tap and source voltages (V_t and V_s , respectively) are measured. Dashed-dotted line: I_t/V_t plotted against the voltage applied to gate A while wire B sustains only one mode. The contributions of the first three modes, δg_i , are indicated. Solid line: three terminal conductance, I_t/V_s , plotted against the voltage applied to gate A. Dashed line: two terminal conductance, g_1 , of the $2 \mu\text{m}$ long wire A, plotted against the voltage applied to gate A. The experimental setups used for the various measurements are sketched. Arrows correspond to current flow direction, and points correspond to a voltage measurement port. The shaded region corresponds to a single mode in both wires A and B.

used as a voltage probe. We find the counterintuitive result of $g_{td,s} = I_t/V_s = 1.49g_0 \approx 2g_2$ (see Fig. 3), while one would naively have expected g_1 . This result is a consequence of the tap current flowing into *both* drain and source wires. The source 2DEG reacts by increasing its electrochemical potential to a value needed to send an equal current in the opposite direction to satisfy the zero source current condition.

In order to interpret our 3T linear response data, we adopt the Landauer scattering approach [2–5], focusing on a single 1D mode. Possible nonideal 2D-1D coupling at the source and drain is modeled, as usual, by a reduced contact emissivity, α . The finite length of the tap, W , leads to a yet smaller tap emissivity: $\alpha T(W)$, where $T(W)$ is the transmission probability from the tap 2DEG into either direction in the first 1DEG mode. Assuming symmetric coupling to both sides, the scattering matrix of the junction depends on these two parameters alone, leading to

$$\begin{cases} I_s = g_0\alpha(V_s - TV_t), \\ I_t = g_0\alpha T(2V_t - V_s). \end{cases}$$

The values of α and T are deduced from two independent measurements. First, α is deduced from the 2T conductance of either wire; $\alpha = g_1/g_0 \approx 0.8$. The transmission T is measured by driving the current from the tap into both the source and the drain and measuring the tap conductance $g_t = I_t/V$ as shown by the

dash-dotted line in Fig. 2. We find $g_t \approx 0.22g_0$, indicating $T = g_t/2g_1 \approx 0.14$ for $W \sim 2 \mu\text{m}$. Without adjustable parameters, we find excellent agreement between all our 3T conductance measurements and this model. For example, the expected overall conductance of both wires in the series is $g_2 = \alpha(1 - T/2)g_0 = 0.74g_0$, as compared to the measured value of $g_2 = 0.75g_0$. Furthermore, the 3T measurement shown in Fig. 3 should yield the same value as a 3T measurement performed by driving the current from the source to the drain and measuring the tap voltage. Both are related by an Onsager symmetry in which current and voltage leads are interchanged. Indeed, we find $g_{sd,t} = 1.51g_0 \approx g_{td,s} \approx 2g_2$ (not shown).

Finally, we address the multimode case. As can be seen in Figs. 2 and 3, the contribution of the i th mode to the overall tap conductance, δg_i , is different for the different modes. This indicates a different coupling between the 2DEG and the various 1DEG modes, as one might expect in general. In order to derive the contribution of the various modes to the overall 2T conductance one would need to determine l_B^{1DEG} and $l_{2D \leftrightarrow 1D}$ for each mode and also the scattering length between modes, to which we have presently no access. In general, one would expect these values to vary, depending on the modes involved. This would lead to a varying height of the 2T conductance steps as successive modes are occupied. In contrast, the observed 2T conductance steps are of *equal* height and *independent* of mode index to within 5%. In a simple model, only a fortuitous, exact cancellation between the mode-to-mode variations in l_B^{1DEG} and $l_{2D \leftrightarrow 1D}$ could explain this result. This behavior is surprising and points to unresolved physics in the transport of multimode 1D wires. However, the simpler single mode case has now been resolved and is understood quantitatively, as shown in the previous section.

In conclusion, we were able to study the coupling between a 2DEG and a 1D wire. Our measurements result in a scattering mean free path of $\sim 6 \mu\text{m}$. These results show that the origin of the previously observed quantized yet nonuniversal conductance is electron scattering across the 2D-1D interface at the contacts. Beyond the well-defined contact geometry of CEO wires, traditional evaporated metal contacts to one-dimensional molecules such as carbon nanotubes, which are conjectured to inject and

remove electrons all along the contact length, may be subject to similar mechanisms.

-
- [1] For a review, see Y. Imry, *Introduction to Mesoscopic Physics* (Oxford University, New York, 1997).
 - [2] R. Landauer, IBM J. Res. Dev. **32**, 306 (1988).
 - [3] M. Buttiker, Phys. Rev. B **33**, 3020 (1986).
 - [4] M. Buttiker, Phys. Rev. Lett. **57**, 1761 (1986).
 - [5] M. Buttiker, IBM J. Res. Dev. **32**, 317 (1988).
 - [6] L. I. Glazman *et al.*, JETP Lett. **48**, 238 (1988).
 - [7] C. W. J. Beenakker and H. von Houten, in *Solid State Physics*, edited by H. Ehrenreich and D. Turnbull, Semiconductor Heterostructures and Nanostructures (Academic Press, New York, 1991).
 - [8] I. Safi and H. J. Schulz, Phys. Rev. B **52**, R17 040 (1995).
 - [9] V. V. Ponomarenko, Phys. Rev. B **52**, R8666 (1995).
 - [10] D. L. Maslov, Phys. Rev. B **52**, R14 368 (1995).
 - [11] Y. Oreg and A. M. Finkel'stein, Phys. Rev. B **54**, 14 265 (1996).
 - [12] A. Y. Alekseev and V. V. Cheianov, Phys. Rev. B **57**, 12 (1998).
 - [13] A. Yacoby *et al.*, Phys. Rev. Lett. **77**, 4612 (1996).
 - [14] L. N. Pfeiffer *et al.*, Microelectron. J. **28**, 817 (1997).
 - [15] A. Yacoby *et al.*, Solid State Commun. **101**, 77 (1997).
 - [16] M. Rother *et al.*, in *Proceedings of the ICPS24*, edited by D. Gershoni (World Scientific, Singapore, 1998).
 - [17] D. Kaufman *et al.*, Phys. Rev. B **59**, R10 433 (1999).
 - [18] Note that while e - e interactions are expected to strongly affect the 2D-1D coupling, the inclusion of e - e interactions is *not* expected to alter the universal quantized conductance in clean wires with ideal contacts [8–12].
 - [19] S. Tarucha, T. Honda, and T. Saku, Solid State Commun. **94**, 413 (1995).
 - [20] B. J. van Wees *et al.*, Phys. Rev. Lett. **60**, 848 (1988).
 - [21] D. A. Wharam *et al.*, J. Phys. C **21**, L209 (1988).
 - [22] We use the tap length for which $T \sim \frac{1}{2}$ to determine $l_{2D \leftrightarrow 1D}$. Similarly, we use the wire length for which the two terminal conductance falls to $\frac{1}{2}$ of its value in [13] to determine l_B . The wires measured in the present work exhibit the same conductance reduction factor as in [13]. We estimate the accuracy of this procedure to be $\sim 20\%$ leading to $\sim 5\%$ uncertainty in the expected value of g_1 .
 - [23] S. J. Tans *et al.*, Nature (London) **386**, 474 (1997).
 - [24] M. Bockrath *et al.*, Nature (London) **397**, 598 (1999).
 - [25] S. Frank *et al.*, Science **280**, 1744 (1998).
 - [26] A. Bachtold *et al.*, Appl. Phys. Lett. **73**, 274 (1998).